Transgenic Mice Expressing Mutated Tyr437His Human Myocilin Develop Progressive Loss of Retinal Ganglion Cell Electrical Responsiveness and Axonopathy With Normal IOP

Tsung-Han Chou,[1] Stanislav Tomarev,[2] and Vittorio Porciatti[1]

[1]Bascom Palmer Eye Institute, University of Miami, Miller School of Medicine, Miami, Florida, United States
[2]Retinal Ganglion Cell Biology Section, Laboratory of Retinal Cell and Molecular Biology, National Eye Institute, National Institutes of Health, Bethesda, Maryland, United States

Correspondence: Vittorio Porciatti, Bascom Palmer Eye Institute, McKnight Vision Research Center, 1638 NW 10th Avenue, Room 201D, Miami, FL 33136, USA; vporciatti@med.miami.edu.

Submitted: May 14, 2014
Accepted: August 1, 2014

Citation: Chou T-H, Tomarev S, Porciatti V. Transgenic mice expressing mutated Tyr437His human myocilin develop progressive loss of retinal ganglion cell electrical responsiveness and axonopathy with normal IOP. *Invest Ophthalmol Vis Sci.* 2014;55:5602–5609. DOI:10.1167/iovs.14-14793

Purpose. To characterize age-related changes of retinal ganglion cell (RGC) function, IOP, and anatomical markers of axon/glia integrity in a transgenic mouse expressing Tyr437His mutant of human myocilin protein.

Methods. Retinal ganglion cell electrical responsiveness was tested with pattern electroretinogram (PERG) in 11 transgenic mice expressing mutated myocilin at different ages over 18 months under ketamine/xylazine anesthesia. Twelve age-matched C57BL/6J mice also were tested as controls. Intraocular pressure was measured with a Tonolab tonometer. Immunohistochemistry for GFAP and neurofilament was performed on dissected optic nerve heads.

Results. In transgenic mice expressing mutated myocilin, the PERG amplitude progressively decreased with increasing age by approximately 50%, whereas the PERG peak latency increased by approximately 40 ms (ANOVA, $P < 0.05$). In contrast, PERGs of young and old control mice had similar amplitudes and peak latencies. In transgenic mice, GFAP staining was more intense and extended than in control mice, and increased with increasing age; neurofilament staining showed swollen and partially degenerated axons in old transgenic mice. The IOP of young transgenic mice was similar to that of control mice and did not significantly change with increasing age.

Conclusions. Transgenic mice expressing mutated human myocilin display progressive age-related changes in RGC electrical responsiveness that are not associated with IOP elevation but are associated with marked astrogliosis and axonopathy. Our results support the view that *MYOC* expression in the optic nerve may impact structural, metabolic, or neurotrophic support to RGC axons, thereby influencing their susceptibility to glaucomatous damage independently of IOP.

Keywords: retinal ganglion cell, pattern electroretinogram, mouse, myocylin, optic nerve, intraocular pressure

Glaucoma is a prevalent group of diseases whose common feature is progressive death of retinal ganglion cells (RGCs), optic nerve degeneration, and eventually blindness.[1,2] The most common form of glaucoma, primary open-angle glaucoma (POAG), is often associated with elevated IOP. However, glaucomatous degeneration of the optic nerve also may develop in individuals without elevated IOP.[3] Despite decades of research, the causative mechanisms of glaucomatous neurodegeneration are still largely unclear.[4–6] Different genes have been identified that account for a small proportion of POAG. In most cases, POAG is inherited as a complex trait.[7,8] The first identified and the most studied gene is *MYOC*, which is highly expressed in the human trabecular meshwork (TM)[9] but also expressed in other ocular tissues, such iris, ciliary body, and optic nerve.[10,11] Several studies have suggested that *MYOC* mutations are associated with 3% to 4% of POAG patient populations worldwide.[12] The role of myocilin in POAG is not fully understood.[11,12] Intracellular accumulation of myocilin aggregates is believed to deteriorate TM function and cause IOP elevation.[13–15] Specific *MYOC* mutations seem to be associated with different levels of IOP elevation and severity of optic neuropathy.[16] However, mice with either deletion of the *Myoc* gene[17] or overexpression of wild-type (wt) *Myoc*[18] have normal IOP and no RGC/axon degeneration, suggesting a gain-of-function property of mutated *MYOC*.[18] Transgenic (Tg) mice expressing the Tyr423His mutant of mouse[19] or Tyr437His human[20] myocilin proteins develop modest IOP elevation and mild RGC loss in the peripheral retina of aged mice. Transgenic mice expressing high levels of mutated human myocilin (Tyr437His) under the control of the cytomegalovirus promoter develop elevated IOP, and early, progressive RGC death and axonal degeneration.[15]

MYOC is also expressed in the retinal pigmented epithelia and optic nerve head and optic nerve astrocytes.[21–26] Thus,

mutated myocilin may potentially contribute to the optic neuropathy. Here we report that Tg mice expressing the Tyr437His mutant of human myocilin protein develop progressive RGC dysfunction associated with marked axonal swelling and astrogliosis in the optic nerve head but not IOP elevation.

Methods

Animals and Husbandry

All procedures were performed in compliance with the ARVO statement for use of animals in ophthalmic and vision research. The experimental protocol was approved by the Animal Care and Use Committee of the University of Miami. Transgenic mice expressing the Tyr437His mutant human myocilin protein have been described.[20] Transgenic founders were crossed to C57BL/6J (B6) mice, and the presence of the *MYOC* mutation in later generations was confirmed by PCR on DNA extracted from tail snips. A total of 11 Tyr437His-positive progenies were available in different age groups: first group, tested at 2 months of age with pattern electroretinogram (PERG)/pattern visually evoked potential (PVEP) and then euthanized for immunohistochemistry; second group, tested serially at 4 and 7 months of age; third group, tested serially with PERG at 10, 13, 16, and 18 months of age. At end point, PVEP was recorded and mice euthanized for immunohistochemistry. Twelve B6 mice (six aged 4 months, six aged 18 months) were tested as controls. IOP data on 13 B6 mice aged 16 and 18 months from a previous study[27] were also included. Mice were maintained in a cyclic light environment (12 hours light at 50 lux and 12 hours dark) and fed with grain-based diet (Lab Diet 500, Opti-diet; PMI Nutrition International, Inc., Brentwood, MO, USA). All measurements (IOP, pattern ERG, visually evoked potentials) were performed under anesthesia. Mice were weighed and anesthetized with intraperitoneal injections (0.5–0.7 mL/kg) of a mixture of ketamine (42.8 mg/mL) and xylazine (8.6 mg/mL). After testing, mice were humanely euthanized and the optic nerves harvested for immunohistochemical analysis.

IOP Measurement

Intraocular pressure was measured with an induction/impact tonometer (Tonolab Colonial Medical Supply, Franconia, NH, USA). The tonometer was fixed in a vertical position to a support stand by means of clamps. The probe tip was aligned with the optical axis of the eye at 1 to 2 mm distance using a magnifier lamp. Three consecutive IOP measures of five readings each were taken and then averaged (15 readings averaged). Local corneal anesthesia was not used because repeated IOP measurements can be performed in nonsedated mice and are not reported to cause obvious corneal damage at biomicroscopic examination. Intraocular pressure readings obtained with Tonolab have been proven to be accurate and reproducible in different mouse strains.[28–31]

Pattern Electroretinogram

Retinal ganglion cell function was assessed by means of the PERG, an electrical signal that specifically depends on RGC integrity[32–34] and is commonly used in human and experimental models of glaucoma and optic neuropathies.[35–37] Pattern electroretinograms were simultaneously recorded from both eyes according to a new paradigm recently described.[38] Anesthetized mice were gently restrained in a custom-made holder that allowed unobstructed vision. The body of the animal was kept at a constant body temperature of 37.0°C using a rectal probe and feedback-controlled heating pad (TCAT-2LV; Physitemp Instruments, Inc., Clifton, NJ, USA). Pupils were natural and had a diameter smaller than 1 mm[39]; eyes were not refracted for the viewing distance because the mouse eye has a large depth of focus.[40,41] A small drop of balanced saline was topically applied as necessary to prevent corneal dryness.

Visual stimuli consisted of contrast-reversing bars with approximately square wave luminance profile[38,42] generated on two custom-made light-emitting diode (LED) tablets (15 × 20 cm). Tablets were made with six parallel rows of 19 LEDs each (LTW-E670DS; LITEON, New Taipei City, Taiwan) separated from each other in a framework of alumina-reflective strips and covered with a diffuser to generate uniform luminance distribution on the surface of each LED row. At the viewing distance of 10 cm, each pattern stimulus covered an area of 56° vertical × 63° horizontal approximately centered on the projection of the optic disk and was invisible to the contralateral eye. The mean luminance of the two LED tablets was 500 cd/m^2 as measured by a photometer (OptiCal OP200-E; Cambridge Research Systems Ltd., Rochester, UK). Contrast was greater than 95%, defined as C = (Lmax – Lmin)/(Lmax + Lmin), where Lmax = luminance of the bright stripes and Lmin = luminance of the dark stripes. Each stimulus contained six horizontal bars (three white and three dark, 0.05 cycles per degree). A spatial frequency of 0.05 cycles per degree and maximum contrast has been previously shown to elicit PERGs of maximal amplitude.[43] A software-controlled digital signal processing (Universal Smart Box; IHSYS, Miami, FL, USA) generated transistor-transistor logic (TTL) signals to trigger the circuit of LED pattern reversal with two unsynchronized stimulation rates (right eye: every 492 ms; left eye: every 496 ms).

Pattern electroretinograms from each eye were simultaneously derived from a common subcutaneous stainless steel needle (Grass, West Warwick, RI, USA) placed in the snout. The reference and ground electrodes were similar needles placed medially on the back of the head and at the root of the tail, respectively. Electrical signals were amplified (10,000 times), band-pass filtered (1–300 Hz, 6 dB/oct), acquired over 183.024 seconds (corresponding to 369 right eye and 372 left eye epochs) and averaged in synchrony with corresponding TTL triggers. The two contrast-reversal frequencies (0.992 Hz and 0.984 Hz) and the averaging time were calculated to obtain a cancellation of the crosstalk between the responses of the right and left eyes, in agreement with previous published theory that enables cross-talk cancellation in simultaneous recordings of multiple generators.[42,44] The recording protocol was based on three consecutive PERG responses, which were automatically superimposed to check for consistency and averaged. As the total recording time was quite long (9 minutes), it was possible that the recording conditions (i.e., anesthesia level) changed over time. As a cautionary measure, the protocol required that successive partial averages were consistent. If not, recording conditions had to be restored and the entire set of partial PERGs recorded again. This occurrence never happened in the present study. As shown in Figures 1A and 1F, PERG waveforms of young Tg and B6 mice consisted of a small negative wave peaking at approximately 50 ms (N1), a positive wave peaking at approximately 80 ms (P1), and a broad negativity peaking at approximately 350 ms (N2).[38] Pattern electroretinogram waveforms were automatically analyzed with MATLAB software (MathWorks, Natick, MA, USA) to identify the major positive (P1) and negative trough (N2). As the small N1 wave could not be unambiguously identified in all PERGs, the amplitude of P1 wave was calculated from baseline to P1 peak; the amplitude on N2 wave was calculated from baseline to N2 trough (the lowest

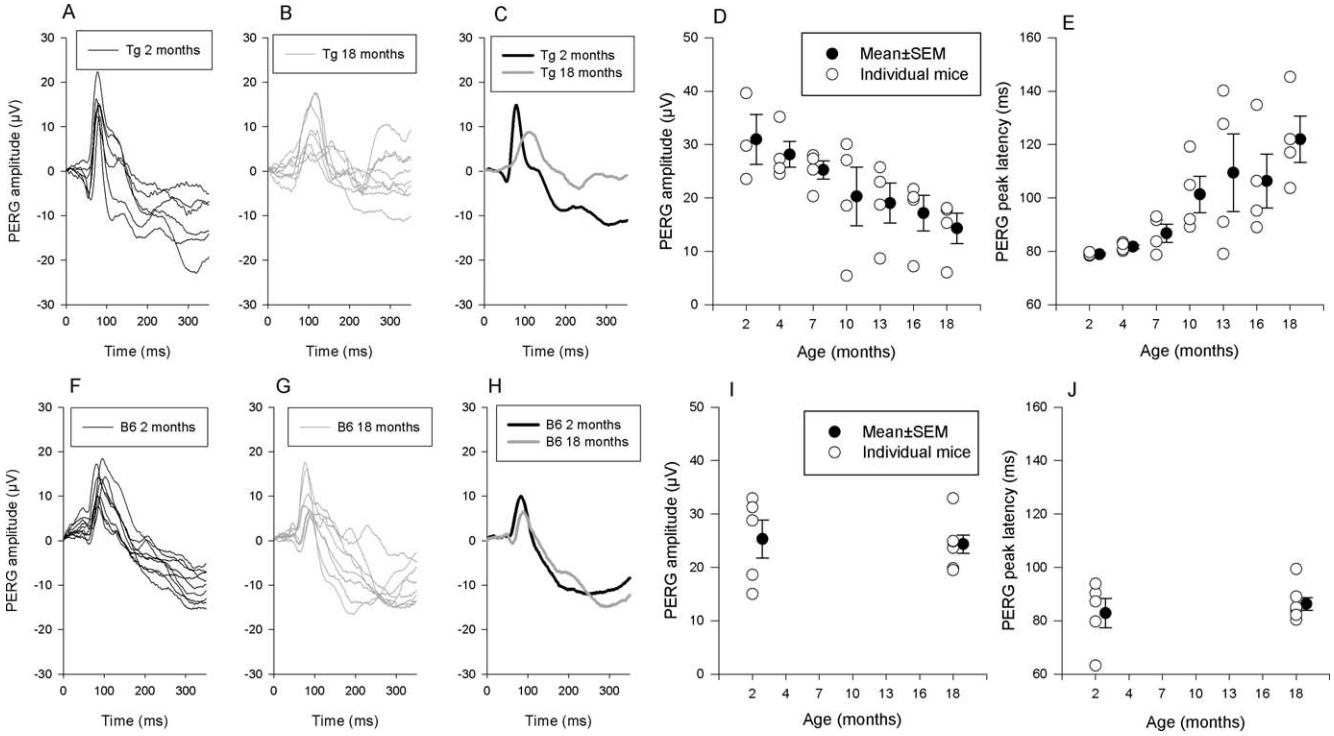

Figure 1. Age-related PERG changes in Tg mice expressing Tyr423His human myocilin (*top*) compared with control C57BL/6J (B6) mice (*bottom*). (**A**, **B**, **F**, **G**) Pattern electroretinogram waveforms recorded in individual eyes of young and old mice (*black*: 2 months old; *gray*: 18 months old). (**C**, **H**) The corresponding grand-average PERG waveforms. Pattern electroretinogram amplitudes (**D**, **E**) and peak latencies (**E**, **J**) as a function of age in Tg mice (*top*) and B6 mice (*bottom*). *Open symbols* represent PERG amplitudes and latencies measured in individual mice (average of the two eyes). *Filled symbols* adjacent to *open symbols* represent the corresponding means ± SEM. Note in (**D**, **E**, **I**, **J**) that in Tg mice the PERG amplitude progressively decreases with increasing age while the PERG peak latency increases. In control mice, the PERG amplitude and peak latency are invariant with age.

negative trough after P1 wave). The peak latency of N2 wave was not considered in the analysis, as its broadness and distortions by noise generated measurement ambiguity. For the purposes of the presents study, the PERG amplitude was defined as the peak-to-trough amplitude of P1-N2 waves, and PERG latency as the peak latency of P1 wave.[38]

Pattern Visually Evoked Potentials

Pattern visually evoked potentials were recorded monocularly (right eye first, left eye second) in response to pattern-reversal stimuli (0.05 cycles per degree > 95% contrast, 1 Hz reversal rate) similarly to the PERG. Pattern visually evoked potentials were recorded from stainless steel screws (shaft length 2.4 mm, shaft diameter 1.57 mm; PlasticsOne, Roanoke, VA, USA) inserted into the skull contralateral to the stimulated eye 2 mm lateral to the lambda suture, which corresponds to the monocular visual cortex.[45,46] Reference and ground electrodes were subcutaneous stainless steel needles in the neck and at the base of the tail, respectively. Pattern visually evoked potential signals were amplified (10,000) band pass filtered (1–100 Hz) and averaged (three consecutive, partial averages of 600 epochs each, whose grand-average constituted the PVEP response). As for the PERG, PVEP signals were automatically analyzed to retrieve the peak-to-trough amplitude and the peak latency of the major positive wave.

Immunohistochemistry

For immunohistochemistry, six mice were perfused with 4% paraformaldehyde, and the eyes with optic nerves were enucleated and immersion-fixed in the same fixative for overnight. The eyes were then rinsed in PBS (pH 7.4) and dissected. The eye with optic nerve was covered in tissue-freezing medium (Tissue-Tek, Torrance, CA, USA) and 10-μm thick frozen sections were cut and mounted on the glass slides (Cat#16004-406; VWR VistaVision HistoBond Microscope Slides; VWR International, Radnor, PA, USA). The sections were permeabilized in the 0.5% Triton X-100 and then immersed in the 0.2% Triton X-100 with goat serum to reduce nonspecific background staining, followed by overnight incubation of the primary antibody at 4°C. Antibodies used included mouse anti-GFAP with Cy3 conjugated (dilution 1:100; EMD Millipore, Temecula, CA, USA) and rabbit antineurofilament (dilution 1:200; Abcam, Inc., Cambridge, MA, USA). After washing in PBS, the sections were incubated with goat anti-rabbit Cy2 secondary antibody (dilution 1:100; Jackson ImmunoResearch Laboratories, Inc., West Grove, PA, USA) for 1 hour at room temperature. The sections were rinsed again, mounted with 4′,6-diamidino-2-phenylindole (DAPI) (H-1200; Vector Laboratories, Inc., Burlingame, CA, USA), and viewed with a confocal microscope (Leica, Exton, PA, USA) (×10).

Statistics

Main analyses were performed by univariate ANOVAs. For analyses of PERG, IOP, and PVEP data, the measurements of the two eyes were averaged and used a single entry.

Results

The main results of this study are summarized in Figure 1. Figures 1A and 1F show that robust PERGs were recordable in

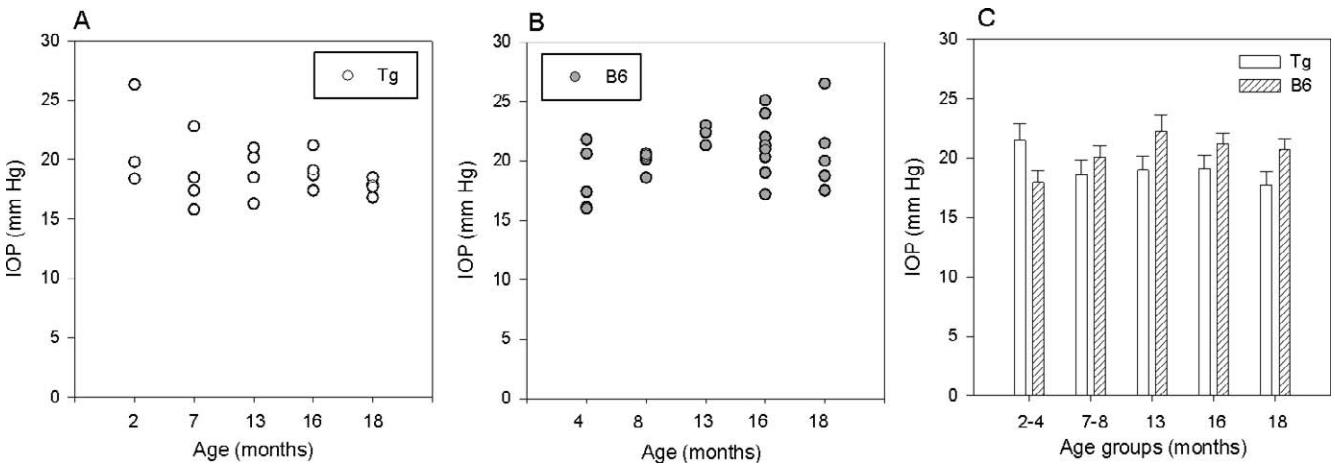

FIGURE 2. Age-related IOP measurements in Tg mice expressing Tyr423His human myocilin (**A**) compared with control C57BL/6J (B6) mice (**B**). Each symbol represents the average of the two eyes. (**C**) Mean ± SEM IOP for each age group of Tg and B6 mice.

all eyes of young Tg and B6 mice and consisted of a small negative wave (N1, ~50 ms), a large positive wave (P1, ~80 ms), and a late negative wave (N2, ~300 ms).[38] No obvious differences were noticeable between young B6 and Tg mice, except a trend to a larger variability in young Tg mice compared with young B6 mice. Pattern electroretinograms of old Tg mice, however, appeared to have reduced amplitude compared with both young Tg mice (Fig. 1A) and old B6 mice (Fig. 1G). Figures 1C and 1H overlay the grand-average PERG waveforms of young and old Tg mice and young and old B6 mice, respectively. It can be noted that the grand-average PERG of old Tg mice, compared with that of young Tg mice, appeared reduced and delayed. No substantial differences were apparent between young and old B6 mice.

The scattergrams displayed in Figures 1D and 1E show peak-to-trough (P1-N2) amplitude and P1 peak latencies as a function of increasing age in individual Tg mice. It can be noted that the PERG amplitude progressively decreased with increasing age while the PERG peak latency increased. The effect was significant, even though the sample was small (ANOVA: PERG amplitude, $P = 0.03$; PERG peak latency, $P = 0.013$). In contrast, Figures 1I and 1J show that the PERG amplitudes and latencies of young and old B6 mice did not show measurable differences.

The scattergrams shown in Figure 2 summarize IOP measurements (average of the two eyes) of Tg and B6 mice of different ages. Figure 2 also includes IOP data on B6 mice aged 16 and 18 months from a previous study.[27] The ranges of IOP values of Tg and B6 mice largely overlapped. Univariate ANOVAs did not did not reveal significant effect of age (Tg: $P = 0.41$; B6: $P = 0.08$). Two-way ANOVA did not reveal significant effect of genotype (Tg versus B6, $P = 0.09$). To investigate the possibility of an IOP role in PERG changes, we performed a multiple regression analysis in Tg mice with either PERG amplitude or peak latency as dependent variable and age and IOP as independent variables. In both cases, age predicted PERG amplitude ($P = 0.03$) and peak latency ($P = 0.008$), whereas IOP did not significantly contribute to the model. In B6 mice, neither age nor IOP were significant predictors of PERG amplitude/peak latency.

Figure 3 compares neurofilament and glial fibrillary acidic protein (GFAP) immunostaining of two young and two older Tg mice in longitudinal sections through the optic nerve head and optic nerve. In young Tg mice, neurofilament staining showed normal appearance of RGC axons in Figures 3A and 3C. Glial fibrillary acidic protein–stained cells were present in the optic nerve fiber layer of the retina, in the nonmyelinated as well as in the myelinated part of the optic nerve. However, GFAP staining was much more extended than that of the control C57BL/6 mice (Fig. 3I).[47] In older Tg mice, neurofilament staining showed swollen and partially degenerated RGC axons (Figs. 3E, 3G). Glial fibrillary acidic protein–stained cells invaded virtually the entire optic nerve head as well as the optic nerve fiber layer of the retina (Figs. 3F, 3H).

Figures 4A and 4B compare the PVEP waveforms of young (2 months old, $n = 3$, six eyes) and older (18 months old, $n = 3$, six eyes) Tg mice in response to the same stimulus used for PERG recording. Signals were recorded by means of screws implanted in the superficial layers of monocular cortices contralateral to the stimulated eyes. In Figure 3C, grand-average PVEPs for each group are shown superimposed. In agreement with previous reports,[45,46] the intracortical PVEP waveform recorded from superficial layers of the visual cortex was characterized by a prominent positive wave peaking at approximately 100 ms, followed by a broad negativity. In older Tg mice, compared with young mice, the grand-average peak-to-trough amplitude appeared reduced and the peak latency of the positive wave appeared delayed. However, the mean PVEP amplitude and peak latency evaluated from individual waveforms (Figs. 4D, 4E) were not significantly different between young and older Tg mice (*t*-test, amplitude, $P = 0.35$; peak latency, $P = 0.5$).

DISCUSSION

As the *MYOC* gene expression is largest in the TM, the focus of most studies has been on the role of myocilin in regulating IOP; however, *MYOC* is also expressed in the optic nerve. This raises the possibility that myocilin plays a structural and functional role in the optic nerve, thereby impacting susceptibility of optic nerve axons to glaucomatous damage. Transgenic mouse models carrying *MYOC* mutations are associated with different levels of IOP elevation and severity of optic neuropathy. Transgenic mice expressing the Tyr437His mutant of human myocilin[20] have previously shown to develop slight IOP elevation associated with moderate RGC loss. Retinal ganglion cell loss may result from IOP-independent, direct effect of mutated myocilin on the optic nerve. The present study investigates age-dependent changes of RGC function in the Tg mice expressing the Tyr437His mutant of human myocilin.

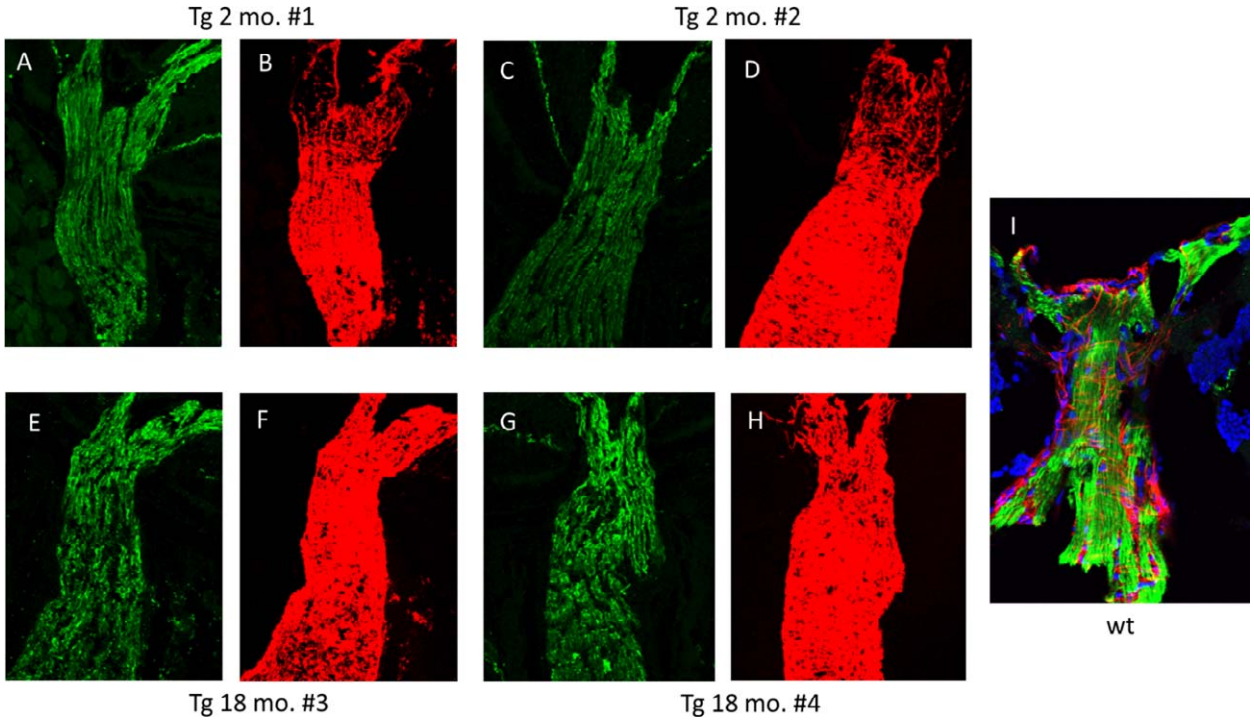

FIGURE 3. Immunostaining for neurofilament (*green*) and GFAP (*red*) in longitudinal sections through the optic nerve head and optic nerve of four different Tg mice expressing Tyr423His human myocilin (*top*, 2-month-olds; *bottom*, 18-month-olds). In older Tg mice (**E**, **G**), RGC axons appear swollen and partially degenerated compared with young Tg mice (**A**, **C**). In both young and old Tg mice, GFAP staining is more intense and widespread than that of representative wt mice (**I**). In older Tg mice (**F**, **H**), GFAP staining is more extended than in young Tg mice (**B**, **D**). In (**I**), GFAP (*red*), neurofilament (*green*), and DAPI staining are shown superimposed.

In agreement with Zhou et al.,[20] our results show that young Tg mice had IOP similar to age-matched C57BL/6J mice. However, Zhou et al.[20] showed a small increase in IOP of 18-month-old Tg mice versus wt littermates using a fiberoptic signal (FTI-10) conditioner equipped with a fiberoptic pressure transducer for IOP measurements. For their study, they used mice of a mixed genetic background that were obtained by crosses of FVB/N founders to C57/BL6 mice for at least five generations. We did not detect IOP changes in the age range of 18 to 22 months using the Tonolab induction/impact tonometer and mice that were crossed to C57/BL6 for more than 10 generations. In the same period, however, the PERG amplitude was progressively reduced by approximately 50%, whereas the PERG peak latency was progressively delayed by approximately 40 ms (increased by ~50%).

Recently, Zode and collaborators[48] induced substantial IOP elevation in wt mice by applying glucocorticoids as eye drops. Intraocular pressure elevation was associated with upregu-

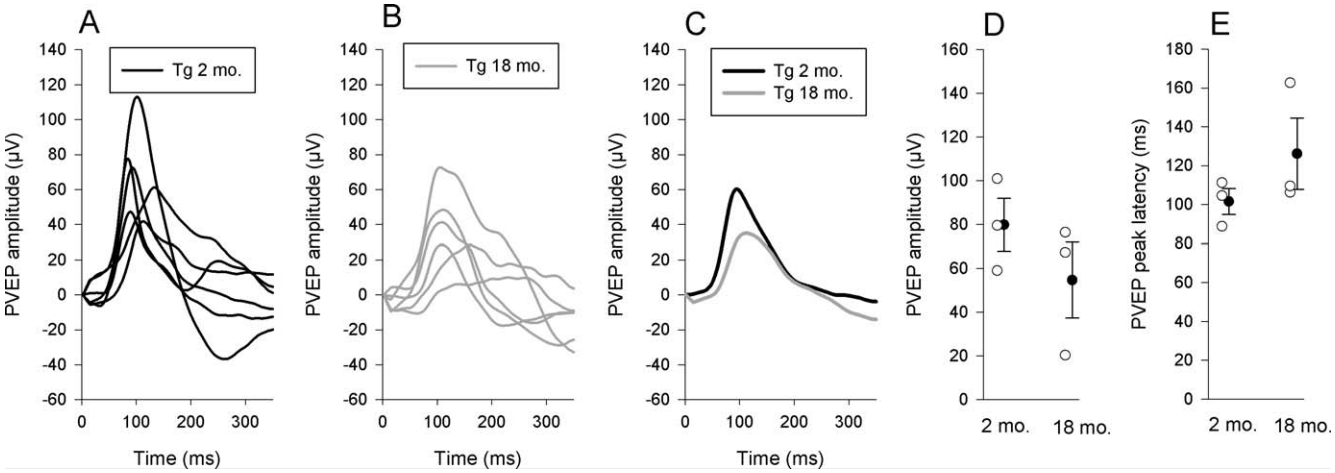

FIGURE 4. Pattern visually evoked potentials in young (**A**) and old (**B**) Tg mice expressing Tyr423His human myocilin ($n = 3$, 6 eyes). (**C**) Grand-average VEP waveforms for young (*black line*) and old (*gray line*) Tg mice. (**D**, **E**) Pattern visually evoked potential amplitudes (**D**) and peak latencies (**E**) measured in individual mice (average of the two eyes). *Filled symbols* adjacent to *open symbols* represent the corresponding means ± SEM. Pattern visually evoked potentials were recorded from a screw electrode implanted in the monocular cortex contralateral to the eye stimulated with a contrast-reversing grating of 0.05 cycles per degree and high contrast.

lation of wt myocilin as well as several other proteins in the TM, and preceded loss of PERG signal and RGC density. The study does not report changes in wt myocilin in the optic nerve. In the present results, mutated myocilin could have contributed directly to loss of PERG signal and structural changes in the optic nerve.

Loss of PERG signal may be caused by RGC loss, dysfunction of viable RGCs, or a combination of both conditions; delay of PERG signal may be caused by viable RGCs that respond in a more sluggish way.[49] The PERG amplitude loss measured in the present Tg mice is similar to that previously reported in DBA/2J mice of 8 months of age[50] when RGC axon degeneration is in its initial stages.[51] An approximately 50% PERG amplitude reduction and approximately 40-ms peak latency delay also can be simulated in normal C57BL/6J mice by lowering the PERG stimulus contrast to 50% of its maximum.[52] This may mean that the slower response of Tg mice results, at least in part, from altered contrast gain of viable RGCs or altered connectivity with preganglionic neurons.

Previous work on Tg mice expressing the Tyr437His mutant of human myocilin[20] has shown moderate (20%) RGC loss in the peripheral retina associated with axonal degeneration at the periphery of the optic nerve and modest IOP elevation. Our results complement and extend previous work[20] showing swelling and degeneration of optic nerve head axons, as well as marked GFAP staining in aged Tg mice, indicating reactive astrogliosis. Axonopathy at the junction between the retina and optic nerve is of particular interest, as it is believed to be the point of origin of glaucomatous neuropathy in humans[53] and mice.[35,54,55] As the PERG signal is also believed to be mainly generated by optic nerve axons in the optic nerve head,[33] axonopathy and astrocytic activation at this level may substantially impair the response.

The magnitude of PERG amplitude loss (50%) appears to exceed the magnitude of RGC loss (20%) reported in previous work.[20] This may mean that surviving RGC/axons were dysfunctional, as has been previously shown in DBA/2J glaucoma.[35,50] Pattern visually evoked potentials of aged Tg mice were modestly reduced by approximately 23% compared with those of young Tg mice. This may mean that surviving RGC axons[20] and dysfunctional, but viable RGC axons are still capable to carrying retinal signals along the geniculo-cortical pathway and contribute to the PVEP response. Compensatory mechanisms may occur in the visual cortex in response to progressive reduction of the retinal output, thereby minimizing VEP loss.[56] It should be also considered that the numerical relationship between topographically matched RGCs and contralateral geniculate relay cells is approximately 3:1.[57] This retina–lateral geniculate nucleus (LGN) convergence may increase the strength of LGN input to the visual cortex and minimize PVEP loss compared with PERG.

In conclusion, the present results show substantial structural and functional age-related changes in Tg mice expressing the Tyr437His mutant of human myocilin, which occur in presence of normal, or close to normal,[20] IOP. We cannot exclude that an IOP level in the normal range may be still a causal factor for axonopathy in susceptible RGC/axons, as in normal tension glaucoma IOP-lowering improves the outcome of the disease.[58] This, however, seems unlikely in the present Tg mouse model, as C57BL/6J-Tyrp1b.GpnmbR150X mice[59] develop the same iris disease as DBA/2J mice and moderate IOP elevation but do not develop age-related glaucomatous changes and PERG loss.[35] Our results support previous views that *MYOC* expression in the optic nerve may impact structural, metabolic, or neurotrophic support to RGC axons, thereby influencing their susceptibility to glaucomatous damage.[22,23] Also, myocilin is expressed and secreted by optic nerve astrocytes, and affects differentiation of oligodendrocytes and myelination of the optic nerve.[26] Reduced myelination of the optic nerve axons may contribute to the axonal damage.

Acknowledgments

Supported by National Institutes of Health (NIH) National Eye Institute Grant RO1 EY019077, NIH Center Grant P30-EY014801, and an unrestricted grant to Bascom Palmer Eye Institute from Research to Prevent Blindness, Inc.

Disclosure: **T.-H. Chou**, None; **S. Tomarev**, None; **V. Porciatti**, None

References

1. Thylefors B, Negrel AD, Pararajasegaram R, Dadzie KY. Global data on blindness. *Bull World Health Organ*. 1995;73:115–121.
2. Quigley H. The number of persons with glaucoma worldwide. *Br J Ophthalmol*. 1996;80:389–393.
3. Friedman DS, Wolfs RC, O'Colmain BJ, et al. Prevalence of open-angle glaucoma among adults in the United States. *Arch Ophthalmol*. 2004;122:532–538.
4. Nickells RW. Retinal ganglion cell death in glaucoma: the how, the why, and the maybe. *J Glaucoma*. 1996;5:345–356.
5. John SW. Mechanistic insights into glaucoma provided by experimental genetics: the Cogan lecture. *Invest Ophthalmol Vis Sci*. 2005;46:2649–2661.
6. Nickells RW, Howell GR, Soto I, John SW. Under pressure: cellular and molecular responses during glaucoma, a common neurodegeneration with axonopathy. *Annu Rev Neurosci*. 2012;35:153–179.
7. Libby RT, Gould DB, Anderson MG, John SW. Complex genetics of glaucoma susceptibility. *Annu Rev Genomics Hum Genet*. 2005;6:15–44.
8. Rao KN, Nagireddy S, Chakrabarti S. Complex genetic mechanisms in glaucoma: an overview. *Indian J Ophthalmol*. 2011;59:S31–S42.
9. Stone EM, Fingert JH, Alward WL, et al. Identification of a gene that causes primary open angle glaucoma. *Science*. 1997;275:668–670.
10. Menaa F, Braghini CA, Vasconcellos JP, et al. Keeping an eye on myocilin: a complex molecule associated with primary open-angle glaucoma susceptibility. *Molecules*. 2011;16:5402–5421.
11. Tamm ER. Myocilin and glaucoma: facts and ideas. *Prog Retin Eye Res*. 2002;21:395–428.
12. Fingert JH, Stone EM, Sheffield VC, Alward WL. Myocilin glaucoma. *Surv Ophthalmol*. 2002;47:547–561.
13. Joe MK, Sohn S, Hur W, Moon Y, Choi YR, Kee C. Accumulation of mutant myocilins in ER leads to ER stress and potential cytotoxicity in human trabecular meshwork cells. *Biochem Biophys Res Commun*. 2003;312:592–600.
14. Liu Y, Vollrath D. Reversal of mutant myocilin non-secretion and cell killing: implications for glaucoma. *Hum Mol Genet*. 2004;13:1193–1204.
15. Zode GS, Kuehn MH, Nishimura DY, et al. Reduction of ER stress via a chemical chaperone prevents disease phenotypes in a mouse model of primary open angle glaucoma. *J Clin Invest*. 2011;121:3542–3553.
16. Shepard AR, Jacobson N, Millar JC, et al. Glaucoma-causing myocilin mutants require the peroxisomal targeting signal-1 receptor (PTS1R) to elevate intraocular pressure. *Hum Mol Genet*. 2007;16:609–617.
17. Kim BS, Savinova OV, Reedy MV, et al. Targeted disruption of the myocilin gene (Myoc) suggests that human glaucoma-

causing mutations are gain of function. *Mol Cell Biol*. 2001;21:7707–7713.

18. Gould DB, Miceli-Libby L, Savinova OV, et al. Genetically increasing Myoc expression supports a necessary pathologic role of abnormal proteins in glaucoma. *Mol Cell Biol*. 2004;24:9019–9025.
19. Senatorov V, Malyukova I, Fariss R, et al. Expression of mutated mouse myocilin induces open-angle glaucoma in transgenic mice. *J Neurosci*. 2006;26:11903–11914.
20. Zhou Y, Grinchuk O, Tomarev SI. Transgenic mice expressing the Tyr437His mutant of human myocilin protein develop glaucoma. *Invest Ophthalmol Vis Sci*. 2008;49:1932–1939.
21. Takahashi H, Noda S, Imamura Y, et al. Mouse myocilin (Myoc) gene expression in ocular tissues. *Biochem Biophys Res Commun*. 1998;248:104–109.
22. Swiderski RE, Ross JL, Fingert JH, et al. Localization of MYOC transcripts in human eye and optic nerve by in situ hybridization. *Invest Ophthalmol Vis Sci*. 2000;41:3420–3428.
23. Karali A, Russell P, Stefani FH, Tamm ER. Localization of myocilin/trabecular meshwork—inducible glucocorticoid response protein in the human eye. *Invest Ophthalmol Vis Sci*. 2000;41:729–740.
24. Noda S, Mashima Y, Obazawa M, et al. Myocilin expression in the astrocytes of the optic nerve head. *Biochem Biophys Res Commun*. 2000;276:1129–1135.
25. Clark AF, Kawase K, English-Wright S, et al. Expression of the glaucoma gene myocilin (MYOC) in the human optic nerve head. *FASEB J*. 2001;15:1251–1253.
26. Kwon HS, Nakaya N, Abu-Asab M, Kim HS, Tomarev SI. Myocilin is involved in NgR1/Lingo-1-mediated oligodendrocyte differentiation and myelination of the optic nerve. *J Neurosci*. 2014;34:5539–5551.
27. Chou TH, Kocaoglu OP, Borja D, et al. Postnatal elongation of eye size in DBA/2J mice compared with C57BL/6J mice: in vivo analysis with whole-eye OCT. *Invest Ophthalmol Vis Sci*. 2011;52:3604–3612.
28. Wang WH, Millar JC, Pang IH, Wax MB, Clark AF. Noninvasive measurement of rodent intraocular pressure with a rebound tonometer. *Invest Ophthalmol Vis Sci*. 2005;46:4617–4621.
29. Pease ME, Hammond JC, Quigley HA. Manometric calibration and comparison of TonoLab and TonoPen tonometers in rats with experimental glaucoma and in normal mice. *J Glaucoma*. 2006;15:512–519.
30. Nissirios N, Goldblum D, Rohrer K, Mittag T, Danias J. Noninvasive determination of intraocular pressure (IOP) in nonsedated mice of 5 different inbred strains. *J Glaucoma*. 2007;16:57–61.
31. Porciatti V, Nagaraju M. Head-up tilt lowers IOP and improves RGC dysfunction in glaucomatous DBA/2J mice. *Exp Eye Res*. 2010;90:452–460.
32. Porciatti V, Pizzorusso T, Cenni MC, Maffei L. The visual response of retinal ganglion cells is not altered by optic nerve transection in transgenic mice overexpressing Bcl-2. *Proc Natl Acad Sci U S A*. 1996;93:14955–14959.
33. Chou TH, Park KK, Luo X, Porciatti V. Retrograde signaling in the optic nerve is necessary for electrical responsiveness of retinal ganglion cells. *Invest Ophthalmol Vis Sci*. 2013;54:1236–1243.
34. Miura G, Wang MH, Ivers KM, Frishman LJ. Retinal pathway origins of the pattern ERG of the mouse. *Exp Eye Res*. 2009;89:49–62.
35. Howell GR, Libby RT, Jakobs TC, et al. Axons of retinal ganglion cells are insulted in the optic nerve early in DBA/2J glaucoma. *J Cell Biol*. 2007;179:1523–1537.
36. Yu H, Koilkonda RD, Chou TH, et al. Gene delivery to mitochondria by targeting modified adenoassociated virus suppresses Leber's hereditary optic neuropathy in a mouse model. *Proc Natl Acad Sci U S A*. 2012;109:E1238–E1247.
37. Enriquez-Algeciras M, Ding D, Mastronardi FG, Marc RE, Porciatti V, Bhattacharya SK. Deimination restores inner retinal visual function in murine demyelinating disease. *J Clin Invest*. 2013;123:646–656.
38. Chou TH, Bohorquez J, Toft-Nielsen J, Ozdamar O, Porciatti V. Robust mouse pattern electroretinograms derived simultaneously from each eye using a common snout electrode. *Invest Ophthalmol Vis Sci*. 2014;55:2469–2475.
39. Nagaraju M, Saleh M, Porciatti V. IOP-dependent retinal ganglion cell dysfunction in glaucomatous DBA/2J mice. *Invest Ophthalmol Vis Sci*. 2007;48:4573–4579.
40. Remtulla S, Hallett PE. A schematic eye for the mouse, and comparisons with the rat. *Vision Res*. 1985;25:21–31.
41. Schmucker C, Schaeffel F. A paraxial schematic eye model for the growing C57BL/6 mouse. *Vision Res*. 2004;44:1857–1867.
42. Chou T-H. *Age-Related Structural and Functional Changes of the Mouse Eye: Role of Intraocular Pressure and Genotype. Biomedical Engineering*. Miami, FL: University of Miami Scholarly Repository; 2011:94.
43. Porciatti V, Saleh M, Nagaraju M. The pattern electroretinogram as a tool to monitor progressive retinal ganglion cell dysfunction in the DBA/2J mouse model of glaucoma. *Invest Ophthalmol Vis Sci*. 2007;48:745–751.
44. Ozdamar O, Bohorquez J. Asynchronized multi-stimulus averaging deconvolution (AMAD) of auditory evoked potentials. Paper presented at: XXIII meeting of the International Evoked Response Audiometry Study Group (IERASG); June 9–13, 2013; New Orleans, LA.
45. Porciatti V, Pizzorusso T, Maffei L. The visual physiology of the wild type mouse determined with pattern VEPs. *Vision Res*. 1999;39:3071–3081.
46. Rossi FM, Pizzorusso T, Porciatti V, Marubio LM, Maffei L, Changeux JP. Requirement of the nicotinic acetylcholine receptor beta 2 subunit for the anatomical and functional development of the visual system. *Proc Natl Acad Sci U S A*. 2001;98:6453–6458.
47. May CA, Lutjen-Drecoll E. Morphology of the murine optic nerve. *Invest Ophthalmol Vis Sci*. 2002;43:2206–2212.
48. Zode GS, Sharma AB, Lin X, et al. Ocular-specific ER stress reduction rescues glaucoma in murine glucocorticoid-induced glaucoma. *J Clin Invest*. 2014;124:1956–1965.
49. Porciatti V, Ventura LM. Physiologic significance of steady-state pattern electroretinogram losses in glaucoma: clues from simulation of abnormalities in normal subjects. *J Glaucoma*. 2009;18:535–542.
50. Saleh M, Nagaraju M, Porciatti V. Longitudinal evaluation of retinal ganglion cell function and IOP in the DBA/2J mouse model of glaucoma. *Invest Ophthalmol Vis Sci*. 2007;48:4564–4572.
51. Libby RT, Anderson MG, Pang IH, et al. Inherited glaucoma in DBA/2J mice: pertinent disease features for studying the neurodegeneration. *Vis Neurosci*. 2005;22:637–648.
52. Porciatti V, Chou TH, Feuer WJ. C57BL/6J, DBA/2J, and DBA/2J.Gpnmb mice have different visual signal processing in the inner retina. *Mol Vis*. 2010;16:2939–2947.
53. Quigley HA. Neuronal death in glaucoma. *Prog Retin Eye Res*. 1999;18:39–57.
54. Soto I, Oglesby E, Buckingham BP, et al. Retinal ganglion cells downregulate gene expression and lose their axons within the optic nerve head in a mouse glaucoma model. *J Neurosci*. 2008;28:548–561.
55. Buckingham BP, Inman DM, Lambert W, et al. Progressive ganglion cell degeneration precedes neuronal loss in a mouse model of glaucoma. *J Neurosci*. 2008;28:2735–2744.

Investigative Ophthalmology & Visual Science

56. Keck T, Mrsic-Flogel TD, Vaz Afonso M, Eysel UT, Bonhoeffer T, Hubener M. Massive restructuring of neuronal circuits during functional reorganization of adult visual cortex. *Nat Neurosci*. 2008;11:1162–1167.

57. Coleman JE, Law K, Bear MF. Anatomical origins of ocular dominance in mouse primary visual cortex. *Neuroscience*. 2009;161:561–571.

58. The effectiveness of intraocular pressure reduction in the treatment of normal-tension glaucoma. Collaborative Normal-Tension Glaucoma Study Group. *Am J Ophthalmol*. 1998;126:498–505.

59. Anderson MG, Libby RT, Mao M, et al. Genetic context determines susceptibility to intraocular pressure elevation in a mouse pigmentary glaucoma. *BMC Biol*. 2006;4:20.

Investigative Ophthalmology & Visual Science